SpaceOps-2023, ID # 462

A Standard Atmospheric Model with Constant Lapse Rates for Titan

Abishek Girish[a]*, Suchithra Selladurai[a], Prasanth A S[a]

[a] *Department of Mechanical Engineering, PSG College of Technology, Avinashi Road, Coimbatore, Tamil Nadu, India 641004,* abishekgirish7@gmail.com
* Corresponding Author

Abstract

The variation of temperature as a function of altitude is of paramount importance in the design and development of space probes and operations. With an increasing number of aerial missions being planned for Titan in search of extraterrestrial life, an atmospheric model will be of substantial utility to scientists and engineers planning such missions. The primary objective of this study is to create a standard atmospheric model for Titan – Saturn's largest moon. The open-source data collected from the Huygens probe is utilized to develop a model that segments the atmosphere into regions of constant lapse rate without significant loss in accuracy. This study employs altitude and temperature to develop the standard atmospheric model. In order to ascertain the optimal change points to segment the atmosphere, four change point detection algorithms are tested. PELT, Fisher-Jenks, piecewise linear regression and the rate of change of gradient algorithms are compared to determine the best suited algorithm. Using mean squared error as the evaluation metric, it is determined that piecewise linear regression with eight segments performs better than competing algorithms. With eight regions, the model is simple enough to evaluate by elementary computations yet robust to accurately capture the true atmospheric parameters. The lapse rates for each of these segments are also ascertained. To validate the outcomes, an atmospheric model for Earth is developed with the algorithm. The results are in good agreement with that of the International Standard Atmosphere. It is envisaged that this generic model can be extended to planets and satellites beyond Titan.

Keywords: Titan, Atmospheric Model, Change Point Detection, Lapse rate, Piecewise Linear Regression

Nomenclature

a	=	Lapse rate (K/m)
T	=	Temperature (K)
h	=	Altitude (m)
$T_{model,i}$	=	Temperature in the i^{th} index as generated by the atmospheric model (K)
$T_{smoothed,i}$	=	Temperature in the i^{th} index of the smoothed model (K)
T_{mean}	=	Mean of temperatures at all indices (K)
R^2	=	Coefficient of determination
p	=	Pressure (Pa)
ρ	=	Density (kg/m^3)
g_0	=	Acceleration due to gravity at the surface (m/s^2)
R	=	Universal gas constant (J/kg-K)
P_0	=	Pressure at the reference altitude (Pa)
ρ_0	=	Density at the reference altitude (kg/m^3)
T_0	=	Temperature at the reference altitude (K)

Acronyms/Abbreviations

HASI	=	Huygens Atmospheric Structure Instrument
ISA	=	International Standard Atmosphere
MAE	=	Mean Absolute Error
MD	=	Maximum Deviation
MSE	=	Mean Squared Error
PELT	=	Pruned Exact Linear Time
SA	=	Standard Atmosphere
SSE	=	Sum of Squares Errors
SST	=	Sum of Squares Total

1. Introduction

Titan is the largest natural satellite of Saturn and the second-largest natural satellite in the solar system. It is located at a distance of approximately 1.2 million km away from Saturn and has a mean radius of around 2574.73 ± 0.09 km [1]. Saturn, the second largest planet in the solar system, is almost 1.4684 billion km away from the Sun. Similar to Earth's moon, Titan is tidally locked in a synchronous orbit with Saturn. This implies that at all times, the same surface of Titan faces Saturn. Titan has an orbital period of 15.945 days around Saturn and 29.458 years around the Sun [2]. Although Titan is at a farther distance from Sun than Earth is, the presence of a dense atmosphere in Titan, necessitates exploring extra-terrestrial life on this satellite. The following sections delineate the notable attributes of Titan which entail an exigent need to develop an atmospheric model for Titan.

1.1 Atmosphere of Titan

Titan is the solitary natural satellite in the solar system with a dense atmosphere. Its atmosphere is primarily composed of Nitrogen (94.2%), Methane (5.65%) and Hydrogen (0.099%) [2]. The deep orange hue in the atmosphere of Titan is attributed to the presence of fine particles of orange-colored organic haze that are created when heavier hydrocarbons mix with nitriles [3]. This haze obscures the surface of Titan for several wavelengths and also causes the atmosphere to exhibit a strong anti-greenhouse effect. Consequently, the surface is vastly cold due to the presence of the haze layer [4].

Titan has a surface temperature of 93.7 ± 0.6 K at 10° S. In contrast to Earth, the poles of Titan are cooler by 2 - 3 K. Further, the temperature of Titan does not vary with the latitude implying that temperature distribution across the satellite remains fairly uniform for the same solar input [5]. The surface pressure in Titan, as observed by the Huygens probe, is 1.467 ± 0.03 bar. This is approximately 1.5 times higher than the surface pressure of Earth [2]. The weak gravitational force on Titan leads to a relatively thicker atmosphere of the order of 10 times that of Earth [6]. Titan has a surface gravity of 1.35 m/s^2 which falls appreciably at higher altitudes. The gas constant for the atmosphere below an altitude of 147 km is calculated to be approximately 295.839 J/kg-K.

The atmosphere of Titan manifests winds primarily due to solar forcing with wind speeds in the troposphere typically ranging from 0.5 to 10 m/s eastward. Higher wind speeds up to 200 m/s have also been observed close to altitudes of 200 km beyond which, the speeds reduce to 60 m/s [7]. Titan manifests several cloud patterns owing to the different processes that create them. Specifically, clouds can be segregated into three categories namely, convective methane clouds, stratiform ethane clouds and high-altitude cirrus clouds [8].

1.2 Morphological features of Titan

The methane cycle of Titan creates morphological features similar to that of Earth. These include channels, lakes and seas. The polar region is characterized by rough, topographically varied bedrock. Three largest seas constitute about 80% of all liquid-filled surfaces on Titan [8]. The presence of liquid methane on the surface of Titan spurs the possible existence of life forms that may be significantly distinct from that of Earth.

1.3 The standard atmosphere and lapse rate

A Standard Atmospheric (SA) model is a mathematical representation of the atmosphere that is used to predict and analyze atmospheric phenomena. This hypothetical model does not account for local weather conditions and ignores factors such as wind and turbulence. SA models presume a set of simplifying assumptions but are accurate enough for several practical purposes. Standard atmospheres specify the change in parameters such as temperature, pressure and density with altitude [10].

SA models play a crucial role in aerospace engineering, aircraft performance and mission planning. These models are used to calculate lift and drag forces besides performance characteristics such as fuel consumption and range. The models are also used to plan the trajectory, deployment of parachutes and other crucial parts of a mission [10].

Lapse rate is a cardinal measure that estimates the change in temperature with altitude. Lapse rate is of three types namely, dry adiabatic, moist adiabatic and the environmental lapse rate. The dry and wet adiabatic lapse rates are derived using laws of thermodynamics, hydrostatic balance and constants relating to the atmosphere and planet/natural satellite [11].

The environmental lapse rate, commonly referred to as the prevailing lapse rate or the ambient lapse rate, is a measure of the actual change in temperature with altitude at a given time and location [11]. The lapse rate, "a" is estimated using Equation 1.

$$a = \frac{dT}{dh} \tag{1}$$

The International Organization for Standardization (ISO) established ISO 2533:1975 as the international standard for Earth's atmosphere, termed the International Standard Atmosphere (ISA). However, to the best of the authors' knowledge, similar standard atmospheric models do not exist for other known planets or natural satellites.

1.4 Rationale for developing a standard atmospheric model for Titan

Titan is of significance to the research community for multifarious reasons. First, Titan is the only natural satellite to exhibit a dense atmosphere. The similarities between the atmospheres of Earth and Titan can possibly yield insights into the evolution of Earth's atmosphere. Second, the existence of planetary features such as mountains, dunes, rivers, and lakes offer the prospects to research on the underlying processes that create them. Missions such as the Dragonfly are dedicated towards the analysis of atmosphere and morphological features that may signify signs of life [12]. Finally, the likelihood of a subsurface ocean with liquid water that can potentially host life on Titan, is of paramount significance for research exploration [13], [14].

With several scientific missions to Titan being planned in the near future, the development of a SA model will benefit scientists and engineers by providing reference values. Therefore, the objective of this study is to create a standard atmospheric model with constant lapse rates for Titan, up to an altitude of 146797 m. As delineated in section 1.1, strong winds restrict effective unmanned operations at higher altitudes. Additionally, it is envisaged that, majority of scientific studies in the future, on the landscape of Titan, will be conducted using drones that operate within this altitude range. This research also aims to exemplify a proof of concept, which may be adapted to atmospheres of other planets and satellites.

2. Material and methods

This research uses data collected by the Huygens module of the Cassini spacecraft. The Cassini orbiter was launched to study Saturn, its rings, and its natural satellites in 1997. The Huygens module designed to investigate Titan, was detached from Cassini on December 25, 2004 and landed on Titan on January 14, 2005. Huygens began its entry phase at an altitude of 1247.7 km and the descent phase at an altitude of 154.4 km. At the latter altitude, the main parachute was deployed and the front shield was jettisoned. The descent with the main parachute lasted until an altitude of 111 km after which the stabilizing drogue was deployed [15]. The descent sequence signifies that the collected data is impervious to the effect of extraneous variables.

The subsequent sections first provide insights into the source of data and then discuss the change point detection algorithms and evaluation metrics employed in this research. Finally, the validation of the optimal algorithm using Earth's atmospheric data is presented.

2.1 Data for the model

The data for the study was gathered from the sensors mounted to the Huygens probe and is presently archived in NASA's public repository. The Huygens Atmospheric Structure Instrument (HASI), a component of the Huygens probe, was an array of sensors utilized to monitor atmospheric conditions. The temperature sensor in this module consisted of two dual element thermometers with an accuracy of 0.5 K and a resolution of 0.02 K. A principal sensor with a wire diameter of 0.1 mm and 2 m length was wound around a Platinum-Rhodium frame. A secondary Platinum wire of diameter 0.02 mm was annealed in the glass on the upper part of the frame. The pressure sensor was a Kiel type pressure probe with capacitive transducers. This instrument had an accuracy of 1% with a resolution of 0.01 hPa [16].

In this study, the open-source data collected by HASI [17] is used to develop models that segment the atmosphere into regions of constant lapse rate without significant loss in accuracy. To segment the data, change points or break points are detected by employing several algorithms.

2.2 Change point and detection algorithms

A change point is defined as a structural change in data. This point is characterized by abrupt or significant changes in the data which signify the beginning of a new segment. Change points segregate data into regions that are statistically different [18]. Change point detection methods are classified into online and offline detection methods. Online methods are used to detect changes in real-time data. These techniques were first developed for industrial quality control and have numerous applications today. On the other hand, offline methods, also termed retrospective change point detections, are employed to detect and interpret changes in recorded data. Typical applications of offline change point detections include signal processing, DNA sequences, spam filtering and climate records. This study employs historically significant offline change point detection techniques to segment the atmosphere.

There exist several algorithms for offline detection of multiple change points such as Dynamic Programming, Pruned Exact Linear Time (PELT), Window-sliding, Binary segmentation, Bottom-up segmentation, Fisher-Jenks algorithm, Rate of change of gradient model and Piecewise Linear Regression. This study explores four widely utilized change point detection algorithms. These four selected algorithms are described below.

2.2.1 Pruned Exact Linear Time

The PELT method is an advancement to the algorithm developed by Jackson, Scargle, et al. [19] with the addition of a pruning step. It assumes that the change points are spread throughout the dataset. PELT has a linear computational time complexity of O(n), where 'n' represents the number of data points. In order to find multiple change points, the algorithm is typically applied iteratively to each partition. This exact method is more accurate than approximate search methods and is faster in comparison to other exact methods. PELT uses a linear cost function that should be minimized. A penalty term (β) in the cost function is used to prevent overfitting. In this algorithm, the pruning step works by neglecting points in that dataset that can never lead to a minima in the cost function [20]. Consequently, PELT is now widely used in climatology, medical imaging and finance [21].

2.2.2 Fisher-Jenks

Fisher-Jenks natural breaks optimization method was initially developed as a data clustering method for choropleth maps. George Frederick Jenks, an American cartographer utilized this method to identify the best clusters by minimizing the variance within clusters and maximizing the variance between clusters. The algorithm has a complexity of $O(n^2K)$ where 'K' represents the number of segments. This algorithm can be used to determine natural breaks in one dimensional data [22] and is widely used to process big data pertaining to demographics [23].

2.2.3 Piecewise Linear Regression

The piecewise regression or segmented regression algorithm by Muggeo was evolved to develop a piecewise regression model when the change points are unknown. The dependent variable is expressed as a function of the independent variable in segments. A parameterization of the 'K' segments is employed in the form of a Heaviside function such that its value is one within the segment and 0 when out of the segment [24]. The goal is to iteratively find change point by means of convergence of a Taylor series linear approximation. Occasionally, Muggeo's algorithm fails to converge on the best solution and instead detects a locally optimal solution [25]. In order to overcome this, the method optionally employs bootstrapping, wherein the algorithm is run on a bootstrapped sample of the data. The piecewise regression algorithm finds extensive usage in medical applications.

2.2.4 Rate of change of gradient

The rate of change of gradient algorithm, specifically designed for this study, relies on detecting abrupt changes in the gradient in order to identify change points. The gradient namely, first order derivative, provides the lapse rate as a continuous function. In order to segment the data, it is required to determine change points where the change in the lapse rate is abrupt. Thus, finding the fourth order derivative is essential. High values, positive or negative, of the fourth order derivatives, manifest the location of change points.

2.3 Evaluation metrics

It is essential to compare all the aforementioned algorithms to identify the best method that is appropriate for the SA dataset of Titan. In order to compare and determine the best suited algorithm, several standard evaluation metrics are utilized. A brief summary of the evaluation metrics is presented below from literature.

2.3.1 Maximum deviation

Error is the difference between the value provided by the model and the smoothed value at the given point. The MD denotes the maximum absolute value of the error of the model from the smoothed data. MD is computed using Equation 2.

$$Max\left(\left|T_{model,i} - T_{smoothed,i}\right|\right) \forall\, i \in \{1,2,\dots,n\} \qquad (2)$$

2.3.2 Mean absolute error

MAE is the average of the absolute error at each index. It measures the spread of the data from the model without considering the amount of deviation from the true value. The mean absolute error is given by Equation 3.

$$\frac{1}{n}\sum_{i=1}^{n}\left|T_{model,i} - T_{smoothed,i}\right| \quad (3)$$

2.3.3 Mean squared error

The MSE is a measure of the average distance of the values in the model to the corresponding values in the true data. The MSE is different from MAE in that, it penalizes values in the model that are farther from the true data by means of squaring the error. The MSE is given by Equation 4

$$\frac{1}{n}\sum_{i=1}^{n}(T_{model,i} - T_{smoothed,i})^2 \quad (4)$$

2.3.4 Coefficient of determination

Commonly referred to as the R^2 value, coefficient of determination is a measure of the variation that is explained by the regression line. R^2 is given by Equation 5.

$$R^2 = 1 - \frac{SSE}{SST} \quad (5)$$

Where, SSE and SST are given by Equation 6 and Equation 7 respectively

$$SSE = \sum_{i=1}^{n}\left(T_{smoothed,i} - T_{model,i}\right)^2 \quad (6)$$

$$SST = \sum_{i=1}^{n}\left(T_{model,i} - T_{mean}\right)^2 \quad (7)$$

All algorithms are implemented using Python, an open-source programming language and its packages.

2.4 Validation of algorithm

In order to validate its functioning, the algorithm that is deemed best suited for Titan's atmosphere is fed with the dataset for Earth's atmosphere to determine the change points. The model is considered to be validated when the change points detected by the algorithm concur with the change points as per the ISA. This step also attests to the performance of the algorithm.

3. Theory and calculation

The atmospheric data, as mentioned in section 2.1, encapsulates information on altitude, pressure, temperature and density. The variables altitude and temperature are used for the development of the SA model. Other parameters such as pressure and density can be computed from the model as elaborated in section 3.2 below, since they are functions of altitude and temperature. Four change point detection methods as delineated in Section 2.2, are employed to segment the atmospheric data into regions of constant lapse rate. Before the implementation of each algorithm, pre-processing of data is essential.

3.1 Deployment of algorithm

Pre-processing involves the elimination of noise from the dataset and transforming the temperature data for equal intervals of altitude. In order to achieve this, a cubic spline interpolation with a smoothing parameter of 500 is utilized. This value for the smoothing parameter was determined iteratively, to be optimal for removing the noise in the data. The smoothed data is used for all further analyses and to compare algorithms.

The PELT algorithm is implemented with the Ruptures library, a python scientific library for change point detection. In this library, three prominent types of cost functions exist namely, L1, L2 and Radial Basis Function (RBF). The L1 cost function is based on the Least Absolute Deviation (LAD) criterion. On the other hand, the L2 cost function is based on the Least Square errors (LS) and is defined as the sum of the squares of the differences between the recorded data and the mean of the corresponding sub-segment. The cost function is iterated over each of the segments detected. RBF is a non-parametric and gaussian kernel-based method for computing the cost function.

The Fisher-Jenks and Piecewise regression algorithms required the number of change points as an input. In this study, the number of change points were iterated in the range between 6 to 11. This range was selected in order to achieve the best trade-off between accuracy, execution time and simplicity. Fisher-Jenks and Piecewise regression use random start values to recursively calculate the most optimal change points. The Fisher-Jenks and piecewise regression algorithms were deployed in Python using the Jenkspy and piecewise_regression libraries respectively.

As elucidated in Section 2.2.4, the rate of change of gradient method relies on finding the points on the curve where the lapse rate varies the most. To accomplish this, the fourth order derivative of the temperature in conjunction with the 'find_peaks' module from the scipy signal library is employed. This module determines the points of local maxima in a given input of 1-D array. The local maxima are computed by comparing the values with neighboring values. The 'find_peaks' module requires a threshold value to be specified. By trial and error, this value was determined to be 0.0002 for detecting all peaks. These peaks indicate the locations of the change points. Fig. 1 illustrates the use of peaks to locate the change points from the fourth order derivative.

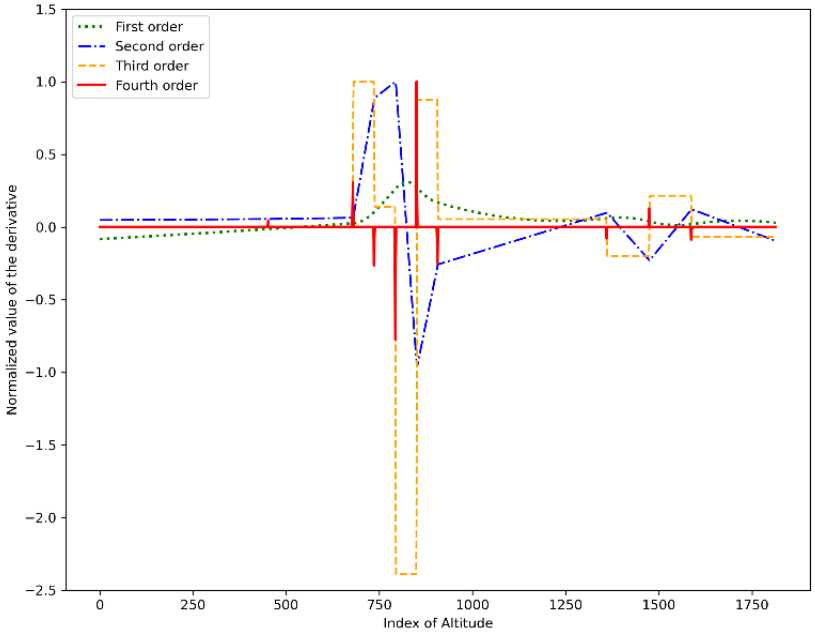

Fig. 1. First, second, third and fourth order derivatives of temperature

Once the change points are detected, the temperature data is linearly interpolated between these change points. The evaluation metrics are then calculated to ascertain the best algorithm. The pressure and density as a function of altitude are finally calculated for this chosen algorithm.

3.2 Evaluation of Pressure and Density

In order to better define the atmospheric conditions, it is necessary to capture the variation of pressure and density with altitude. The hydrostatic and the ideal gas equations shown in Equations 8 and 9 respectively, can be utilized to develop pressure and density as a function of altitude [10]. In this context, the acceleration due to gravity is assumed to be constant throughout the atmosphere.

$$dp = -\rho g_0 \, dh \tag{8}$$

$$p = \rho R T \tag{9}$$

Using lapse rate and integrating with temperature yields Equation 10 and Equation 11 with pressure and density respectively as a function of altitude.

$$P = P_0 \left[\frac{T}{T_0}\right]^{-\frac{g_0}{aR}} \tag{10}$$

$$\rho = \rho_0 \left[\frac{T}{T_0}\right]^{-\left[\frac{g_0}{aR}+1\right]} \quad (11)$$

T can be estimate with T_0 using Equation 12.

$$T = T_0 + a(h - h_0) \quad (12)$$

4. Results and Discussion

As elucidated in section 3.1, all algorithms are tested within a range of change points between 6 and 11. The variation in the values of the evaluation metrics with the increase in number of change points was analysed to select the desired number of change points. The methodology adopted for this change point selection is illustrated below for Piecewise Linear Regression model.

The MSE and MD values were initially evaluated by varying the number of change points from 6 to 11. Fig. 2 shows the variation of MSE and MD as a function of the change points. It can be inferred that both the MSE and MD fall sharply from the 6th to the 7th change point.

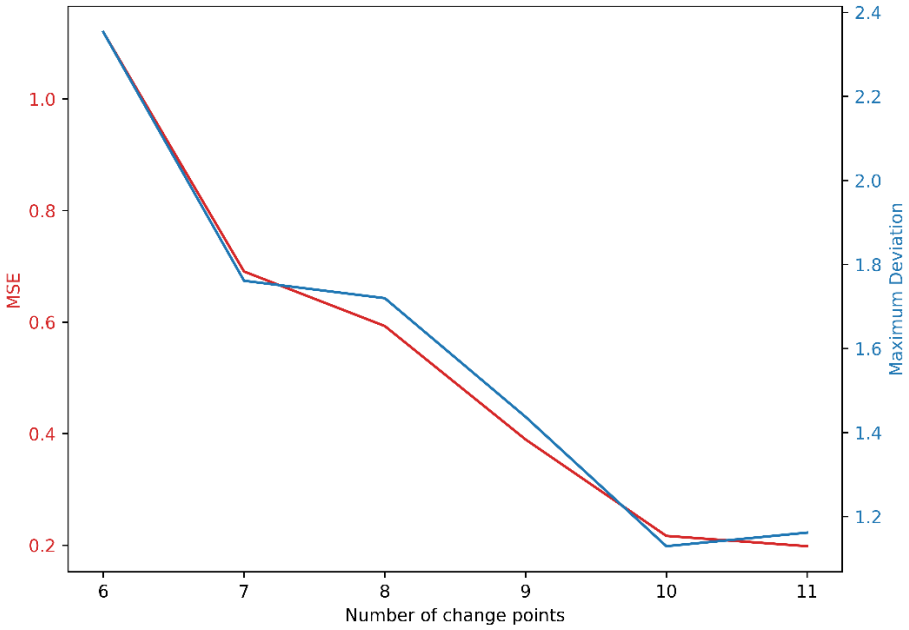

Fig. 2. Variation of MSE and MD with change points for Piecewise Linear Regression Model

A significant improvement in the model fit is observed when the number of change points is increased from 6 to 7. However, the model fit diminishes after the 7th change point. Additionally, adding more change points leads to only a minuscule change in the values of MSE and MD. The MSE values change by less than 0.15. This signifies that the model only performs marginally better beyond the 7th change point. Typically, fewer change points lead to reduced complexity. Therefore, the model with the number of change points as 7, is selected as the optimal model. This implies that 7 change points is ideal for the piecewise linear regression model. A similar procedure is adopted for the other algorithms and number of change points detected are tabulated in Table 1. Subsequently, atmospheric models are plotted by utilizing each algorithm.

Table 1. Algorithms and optimal number of change points

Algorithm	Number of change points
Pruned Exact Linear Time (PELT) (Cost function = L1)	10
Fisher Jenks Natural Breaks Algorithm	10
Piecewise Linear Regression	7
Rate of change of gradient	9

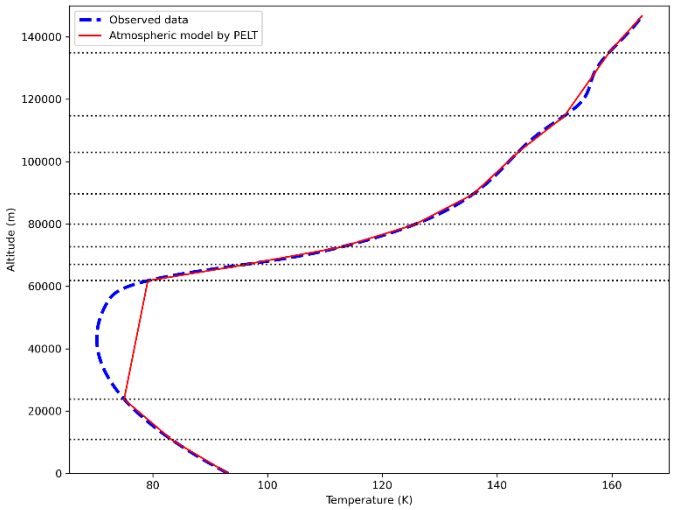

Fig. 3. Atmospheric model developed using the PELT algorithm

A graph of the atmospheric model produced by the PELT algorithm with 10 change points and 11 segments is shown in Fig. 3. It can be inferred that the algorithm has performed well for regions lower than altitude of 23833.3 m and higher than 61805.01 m. Moreover, the algorithm is distinctly sensitive in the altitude range between 61805.01 m and 79982.9 m. Furthermore, the PELT algorithm was tested using different cost functions and the L1 function was observed to be the most appropriate in terms of identifying optimal change points with the least MSE. This algorithm exhibits a maximum deviation of 7.103 K at an altitude of 47262.65 m.

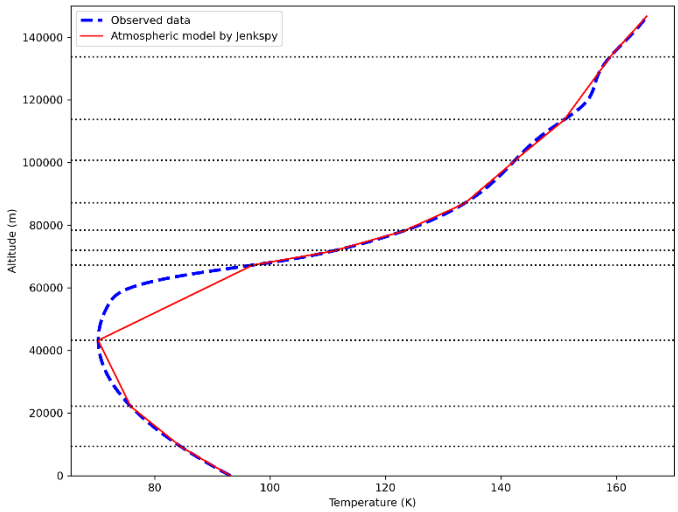

Fig. 4. Atmospheric model developed using the Fisher-Jenks algorithm

Fig. 4 shows a graph of the atmospheric model developed using the Fisher-Jenks algorithm with 10 change points and 11 segments. It can be inferred that the model performance is adequate in the altitudes below 43223.1 m and above 67217.9 m. However, the model fit between 43223.1 m and 67217.9 m is poor. Additionally, in comparison with other models, Fisher-Jenks exhibits the highest MSE and a maximum deviation of 13.29 K at 59058.12 m.

Fig. 5 shows a plot of the atmospheric model developed using the piecewise linear regression algorithm with 7 change points and 8 segments. The model is more sensitive in the mid region between an altitude of 56349.5 m and 84068.8 m. With the exclusion of the mid region, it can be seen that the break points are spaced out more evenly to model the variations better compared to other algorithms. With the value of MSE being 0.7265, and the maximum deviation of smoothed temperature from the linearly regressed model being 1.761 K at an altitude of 77560 m, this model is precise in capturing the temperature variation with respect to the altitude.

Fig. 6 depicts a plot of the atmospheric model developed using the rate of change of gradient algorithm with 9 change points and 10 segments. The change points for this algorithm are found by locating the peaks in the 4th order derivative of temperature. Similar to the PELT algorithm, it can be seen that this model is highly sensitive in the mid region from 55180.1 m to 64390.3 m. The fit of the model exacerbates in the altitude range between approximately 73519.6 m and 110198.7 m. Furthermore, the model has a MSE of 7.3060 and a maximum deviation of 6.653 K at an altitude of 86527.01 m.

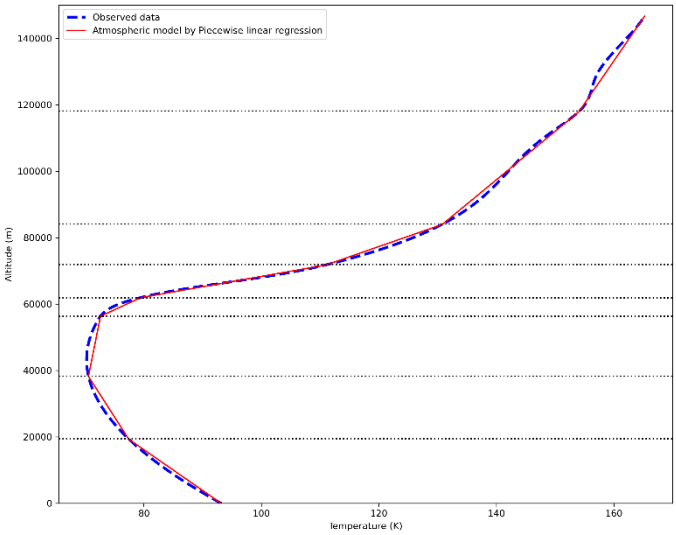

Fig. 5. Atmospheric model developed using the Piecewise Linear Regression algorithm

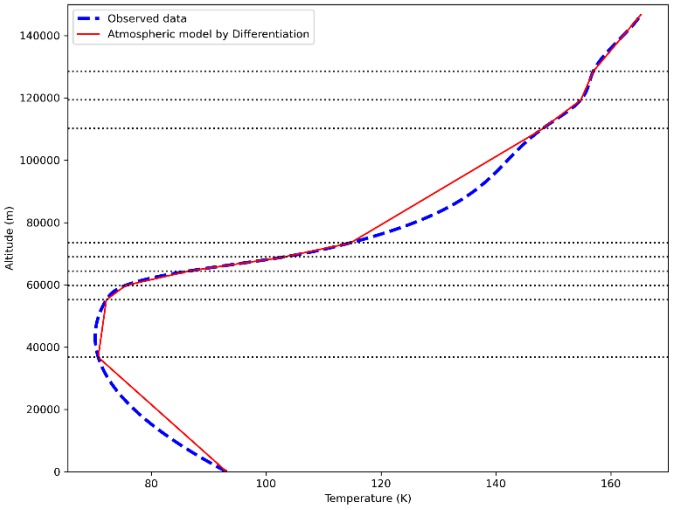

Fig. 6. Atmospheric model developed using the rate of change of gradient algorithm

Table 2 provides a summary of the evaluation metrics of each model along with their ranks. The ranking of models is determined by comparing the MSE values. It can be observed that the R^2 values of all the models are at least 0.98 implying that all the models are statistically significant. As can be inferred from Figs. 3 to 6 and Table 2, piecewise linear regression performs better than competing models compared in this study. It is significant to note that, although the piecewise linear regression model uses only 7 change points, it achieves better results than competing models. Subsequently, the pressure and density as a function of altitude are estimated for the atmospheric model developed using the piecewise linear regression algorithm with 7 change points.

Fig. 7(a) depicts a plot of pressure vs altitude that compares model performance with the original dataset. Fig. 7(b) shows a similar plot of density vs altitude. It can be observed that the piecewise regression model with 7 change points accurately captures the observed pressure and density data with a maximum percentage deviation of 0.56% for pressure at an altitude of 13411.28 m and 1.56% for density at an altitude of 7432.76 m.

Table 2. Evaluation metrics for the algorithms

Algorithm	Number of change points	MSE	MAE	MD	R^2	Rank
Piecewise Linear Regression (Python)	7	0.7265	0.70867	2.30086	0.99941	1
Rate of change of gradient	9	7.30602	1.84193	6.65327	0.99372	2
Pruned Exact Linear Time (PELT) (Cost function = L1)	10	7.89517	1.59672	7.103	0.99308	3
Fisher Jenks Natural Breaks Algorithm	10	13.55779	1.71285	13.29917	0.98817	4

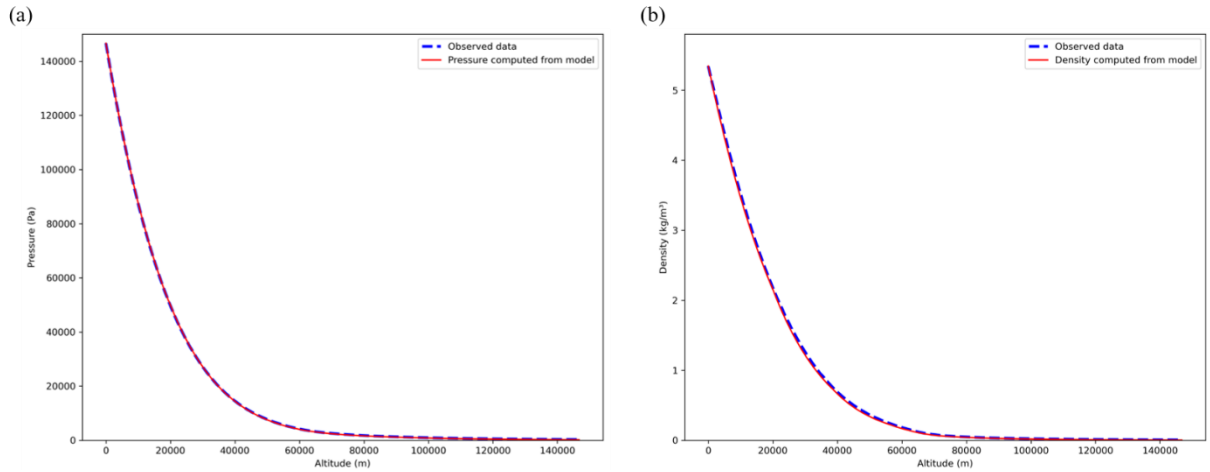

Fig. 7. (a) Pressure and (b) Density as a function of altitude

In order to validate the performance of piecewise linear regression algorithm with other atmospheres, segmentation was performed on the established atmospheric model of Earth using the algorithm. A comparison between the segmented model of the Earth's atmosphere and ISA along with the smoothed data is shown in Fig. 8. As can be inferred from Fig. 8, the model was effective with an MSE of 2.023 and a maximum deviation of 3.474 K. Table 3 exhibits the change points obtained from the piecewise regression model against the change points defined by ISA.

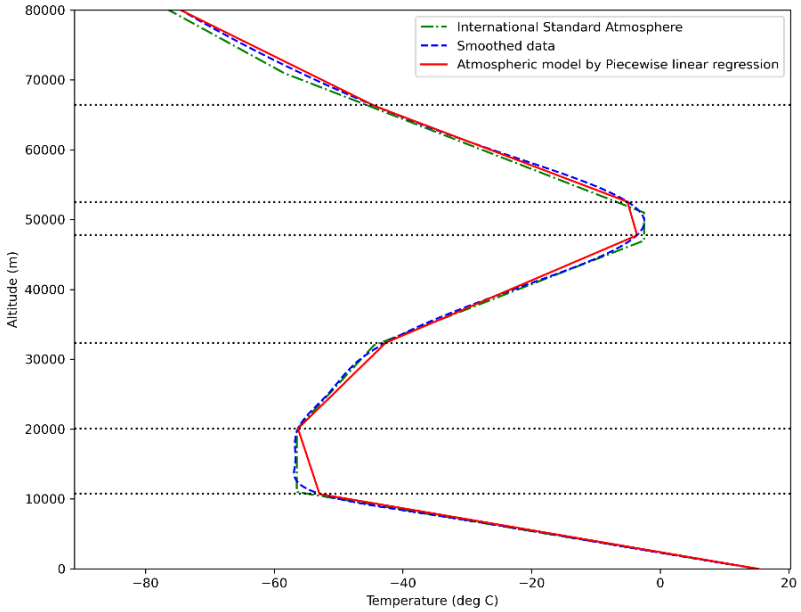

Fig. 8. Piecewise linear regression on Earth's atmosphere compared to the ISA

Table 3. Change point defined by ISA and that derived from the model for Earth

Change point number	Altitude according to ISA (m)	Altitude as derived from model (m)
1	11000	10762
2	20000	20106
3	32000	32321
4	47000	47787
5	51000	52000
6	71000	66443

The results demonstrate that the piecewise regression model yields optimal results for the atmospheric models of both Titan and Earth. A summary of the segments and the lapse rates for Titan's atmospheric model is therefore computed and tabulated in Table 4. It is envisaged that the constant lapse rates identified for the different altitude regimes will be of profound use in unmanned space flights to Titan in the near future.

Table 4. Altitude range and lapse rates for Titan

Segment Number	Altitude Range (m)	Lapse rate (K/km)
1	0 - 19470.59	-0.81062
2	19470.59 - 38294.86	-0.36095
3	38294.86 - 56311.23	0.113188
4	56311.23 - 61885.80	1.203102
5	61885.80 - 71903.86	3.185938
6	71903.86 - 84103.28	1.610176
7	84103.28 - 118116.24	0.683603
8	118116.24 - 146716.21	0.388825

5. Conclusion

Overall, this paper expounds a generic methodology to create atmospheric models. The process involves pre-processing the data by means of smoothing, using a suitable change point detection algorithm and linear interpolation between these change points. The piecewise regression model provides an optimal result amidst other methods considered in this study, such as PELT, Fisher-Jenks, and rate of change of gradient for segmenting Titan's atmospheric data. Moreover, determining the optimal number of change points for any model involves a trade-off between simplicity, time for execution and accuracy of the model. In order to validate the results on a distinct dataset, the selected model is tested on the atmospheric data of Earth. The change points provided by the piecewise regression model are in good agreement with the existing change points of the ISA data. Therefore, this segmentation model can be used for future analysis of new datasets to create atmospheric models.

Such atmospheric models encompass regions of constant lapse rate and will be of profound use in space flight planning due to the intrinsic simplicity of the model. These space flights can survey geological and meteorological characteristics of planets and their satellites. Since quantities such as lift, drag, Mach number and Reynold's number are functions of temperature and density, atmospheric models can be extensively utilized in space vehicle design. In summary, creating SA models can prove helpful in estimating the pressures, temperatures and densities used in the design of space propulsion systems.

6. Future Work

The data analyzed in this research pertains to one geographic location of Titan at a particular time. To enhance the model, data from different regions need to be gathered at different points in time. Additionally, in this study, the SA model has been developed only till an altitude of approximately 146 km. Further studies are essential to verify if the present model can be extended to the upper atmosphere without loss in accuracy. The SA model also assumes a constant value for the acceleration due to gravity. This assumption may impact the accuracy of the model when applied to higher altitudes. With advancements in computation, several other optimization techniques can be explored to create SA models. Future studies can also explore whether atmospheres of other planets can be modeled with the algorithm suggested by this study.

References

[1] Zebker, H. A., Stiles, B., Hensley, S., Lorenz, R., Kirk, R. L., Lunine, J., Size and Shape of Saturn's Moon Titan, Science 324 (2009) 921–923.

[2] Catling, D. C., and Kasting, J. F. *Atmospheric Evolution on Inhabited and Lifeless Worlds.* Cambridge University Press, 2017.

[3] Teanby, N., Cassini at Titan: The Story so Far, Astronomy *and Geophysics* 46 (2005) 5.20-5.25.

[4] McKay, C. P., Pollack, J. B., and Courtin, R., The Greenhouse and Antigreenhouse Effects on Titan, *Science 253 (1991) 1*118–1121.

[5] Hörst, S. M., Titan's Atmosphere and Climate, *Journal of Geophysical Research: Planets* 122 (2017) 432–482.

[6] Davis, P., Dunford, B., and Boeck, M. In Depth | Titan – NASA Solar System Exploration. 26 January 2023, https://solarsystem.nasa.gov/moons/saturn-moons/titan/in-depth/. (accessed 26.01.23)

[7] Bird, M. K., Allison, M., Asmar, S. W., Atkinson, D. H., Avruch, I. M., Dutta-Roy, R., Dzierma, Y., Edenhofer, P., Folkner, W. M., Gurvits, L. I., Johnston, D. v., Plettemeier, D., Pogrebenko, S. v., Preston, R. A., and Tyler, G. L., The Vertical Profile of Winds on Titan, *Nature 438 (2005)* 800–802

[8] Tsai, I. C., Liang, M. C., and Chen, J. P., Methane–Nitrogen Binary Nucleation: A New Microphysical Mechanism for Cloud Formation in Titan's Atmosphere, *The Astrophysical Journal 747 (2012)* 1-7.

[9] Hayes, A. G., The Lakes and Seas of Titan, Annual Review of Earth and Planetary Sciences 44 (2016) 57–83.

[10] Anderson, J. D., and Bowden, M. L, Introduction *to Flight*, McGraw Hill, 2022.

[11] Frederick, J. E., *Principles of Atmospheric Science*, Jones and Bartlett Publishers, 2008.

[12] Northon, K, NASA's Dragonfly Mission to Titan Will Look for Origins, Signs of Life, 28 June 2019, https://www.nasa.gov/press-release/nasas-dragonfly-will-fly-around-titan-looking-for-origins-signs-of-life. (accessed 23.01.23)

[13] Baland, R. M., van Hoolst, T., Yseboodt, M., and Karatekin, Ö., Titan's Obliquity as Evidence of a Subsurface Ocean?, *Astronomy & Astrophysics* 530 (2011) 1-6.

[14] Lunine, J. I., Ocean Worlds Exploration, *Acta Astronautica* 131 (2017) 123–130.

[15] Kazeminejad, B., Atkinson, D. H., Pérez-Ayúcar, M., Lebreton, J. P., and Sollazzo, C., Huygens' Entry and Descent through Titan's Atmosphere—Methodology and Results of the Trajectory Reconstruction, *Planetary and Space Science* 55 (2007) 1845–1876.

[16] Fulchignoni, M., Ferri, F., Angrilli, F., Bar-Nun, A., Barucci, M. A., Bianchini, G., Borucki, W., Coradini, M., Coustenis, A., Falkner, P., Flamini, E., Grard, R., Hamelin, M., Harri, A. M., Leppelmeier, G. W., Lopez-Moreno, J. J., McDonnell, J. A. M., McKay, C. P., Neubauer, F. H., Pedersen, A., Picardi, G., Pirronello, V., Rodrigo, R., Schwingenschuh, K., Seiff, A., Svedhem, H., Vanzani, V., and Zarnecki, J. *The Characterisation of Titan's Atmospheric Physical Properties by the Huygens Atmospheric Structure Instrument (HASI), The Cassini-Huygens Mission (2*003) 395-431.

[17] Huber, L., and Chanover, N. Huygens Atmospheric Structure Instrument. 25 August 2022, https://pds-atmospheres.nmsu.edu/data_and_services/atmospheres_data/Huygens/HASI.html. (accessed 23.01.23).

[18] Burg, G. J. J. van den, and Williams, C. K. I., An Evaluation of Change Point Detection Algorithms., arXiv:2003.06222 stat.ML (2003) 1-39.

[19] Jackson, B., Scargle, J. D., Barnes, D., Arabhi, S., Alt, A., Gioumousis, P., Gwin, E., Sangtrakulcharoen, P., Tan, L., and Tsai, T. T., An Algorithm for Optimal Partitioning of Data on an Interval, *arXiv:math/0309285 math.NA (*2004) 1-4.

[20] Killick, R., Fearnhead, P., and Eckley, I. A. Optimal Detection of Changepoints with a Linear Computational Cost, *Journal of American Statistical Association 107 (2012)* 1590–1598.

[21] Dorcas Wambui, G., Anthony Waititu, G., and Wanjoya, A., The Power of the Pruned Exact Linear Time(PELT) Test in Multiple Changepoint Detection, *Science Publishing Group* 4 (2015) 586.

[22] Coulson, M. R. C., In the Matter of Class Intervals for Choropleth Maps: With Particular Reference to The Work of George F Jenks, *Cartographica* 24 (2006)16–39.

[23] Rey, S. J., Stephens, P., and Laura, J., An Evaluation of Sampling and Full Enumeration Strategies for Fisher Jenks Classification in Big Data Settings., *Transactions in GIS* 21 (2017) 796–810.

[24] Muggeo, V. M. R., Estimating Regression Models with Unknown Break-Points, *Statistics in Medicine* 22 (2003) 3055–3071.

[25] Pilgrim, C., and Robles, G. A., Piecewise-Regression (Aka Segmented Regression) in Python., *Journal of Open-Source Software* 6 (2021) 1-4.